

---

## Detection of surface defects on sheet metal parts by using one-shot deflectometry in the infrared range

Zoltán Sárosi, Wolfgang Knapp, Andreas Kunz, Konrad Wegener  
IWF, ETH Zurich, Switzerland

---

### ABSTRACT

The early detection of surface defects on raw sheet metal parts is a critical problem in the automotive industry. Typical defects like dents, bumps and waviness are invisible at the early production stages because of the parts' rough surfaces. The defects become visible and disturbing only after the later production steps, in which the parts get painted and varnished, meaning that they become specular reflecting. The later the defect gets detected, the more the correction will cost. Currently, the raw sheet metal parts are only randomly tested by special, trained experts, which means subjective and qualitative results. To overcome this problem, we propose a method that can be used on-line on each part directly at the production line. The system employs a one-shot deflectometry method in the infrared range. At sufficiently long wavelengths, the sheet metal's surface becomes specular reflecting, thus enabling the use of the deflectometry method. For this method, a device capable of displaying a reference pattern at the infrared wavelengths was developed. This single infrared reference pattern is reflected from the surface of the raw sheet metal object and the reflected image is captured by a thermo-camera. The distortion of the reflected pattern due to the surface's geometry and defects is analyzed by the Fourier-transform method. Due to the single exposure method, vibrations during the measurement are not disturbing and the alignment problem, that is characteristic for multi-exposure methods, is nonexistent in this case.

### INTRODUCTION

Quality control of car-body parts in the automotive industry is of critical importance, since the competition between the manufacturers is always getting sharper. The first impression from a car is made by the observation of the exterior appearance. A flawless exterior with smooth surfaces and edges suggest technical superiority. Customers intentionally look for objects in the environment with a linear texture e.g. fluorescence light tubes, and observe the course of reflection lines on the surface of the body. Studies [1] showed that dents and bumps with already ten micrometers depth and several millimeters lateral dimension can be visually perceived on a varnished car-body. In the early production stages, these small defects are hidden from the human observer, because of the rough, dull surface quality of the raw parts. They become visible and disturbing only after the later production steps, in which the parts get painted and varnished, meaning that they become specular reflecting. With each production step, the price of the part increases, due to the additionally invested work, time and material. The later the defect gets detected, the more the correction will cost.

Currently, the raw sheet metal parts are only randomly tested using conventional measurement methods e.g. form gauge, haptic test by special experts, abrasive stripping of the parts and observation of the scratch marks, or highlighting the surface with special oil that allows observing the reflection lines due to oil film's specularly. All these methods are time consuming and based on human observations, entailing subjectivity, lack of repeatability and quantitativity. Coordinate measurement machines (CMM) can, though, produce accurate, quantitative results, but due to the mechanical contact with the flexible part, the results are biased and the measurement process can take several ten minutes in case of many points, not to mention the need for special environmental conditions. Laser-triangulation techniques have an advantage in measurement speed over CMMs, though measurement of a surface still needs several scanning steps. Fringe projection method can simultaneously capture millions of surface points of light colored, homogeneous, texture-less, diffuse reflecting objects, but glossy, metallic surfaces need to be treated by a special chalk-spray prior the measurement to reduce gloss, otherwise it generates noisy or no measurement data at all (see Table 1). Deflectometry is a white light, whole field method, which is appropriate for the form measurement of specular, highly reflecting objects e.g. mirrors, lenses, or varnished car-body parts, but raw, dull surfaces have to be treated with oil in order to generate shininess (see Table 1).

The need for surface treatment like highlighting oil or chalk spray hinders the application of these methods in the mass production, as the parts have to be cleaned, homogeneously treated by the substance, which again has to be removed after the measurement. Due to the need for excessive use of such substances, these methods are neither economical nor ecological.

A new, whole-field measurement method is needed, which can measure a high number of points simultaneously of an untreated, raw, metal sheet, and can detect and numerically evaluate small deviations of the surface.

Measurement signals		
		Reflection property of the object's surface in visible light spectrum
		diffuse   specular
Measurement method	fringe-projection	o.k. ← changing property with surface treatment → noisy
	deflectometry	noisy ← changing property with surface treatment → o.k.

Table 1: Surface treatments for fringe-projection and deflectometry method

### DEFLECTOMETRY METHOD

Deflectometry method is actually an advanced, computer aided version of the human observation process of specular objects which we described previously. The method was first proposed by Ritter and Hahn [2] as an advanced version of the reflection moiré method. A reference pattern, usually consisting of several parallel stripes, is captured by a camera as being reflected from the test surface. Often, instead of the stripe pattern a cosine intensity patten is used, in order to increase the resolution. The pattern in the camera images is distorted due to the 3D geometry of the test object (see Figure 1a). Irregularities in the specimen's geometry deflect the reflected light beams by a twofold angle difference (see Figure 1b), which makes this method very sensible to local slope changes of the surface. Since most surface defects like dents, bumps and waviness have small height difference, which is distributed in a relatively large area, thus they are rather slope irregularities in the first place, the deflectometry method is ideal for their detection.

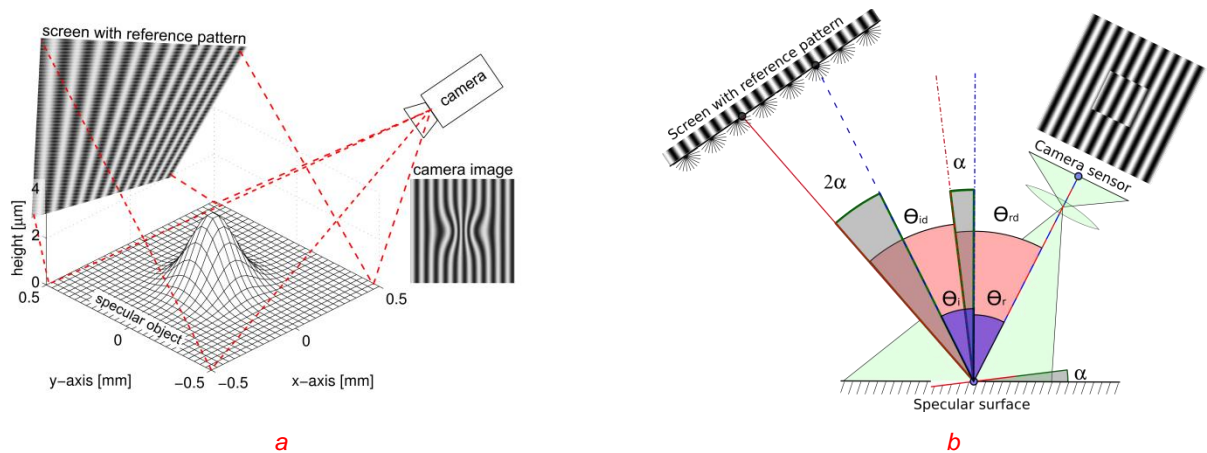


Figure 1. Deflectometry method: a. 3D illustration object geometry is exaggerated in z direction for the illustration, b. 2D model

Deflectometry method, unlike triangulation based techniques, can directly measure the surface's slope, that is a derivate of the height in case of continuous surfaces. If positions of the screen, object and the camera are known, the 3D height map of the object can be reconstructed if required, by integration of the slope values. Rose et. al [3] describe the advantages of the slope measuring techniques, primarily the deflectometry method, over the height measuring ones, in field of surface characterization and defect detection: since the

height data are obtained through the integration of the slope data, this method acts as a low pass filter, reducing the measurement noise.

Deflectometry is the appropriate method for the detection of geometry defects on highly specular, mirroring surfaces (see Figure 2a) like optical components: lenses, mirrors [6], reflectors [7], or automotive glass [8], or varnished car-body [9].

The sensitivity of deflectometry system can be easily amplified by either increasing the number of the pattern's stripes or moving the screen backwards, away from the object. The achievable depth resolution of the deflectometry method is in the sub- $\mu\text{m}$  range, even nm range is reported to be reachable [3,10].

### PATTERN EVALUATION

For the evaluation of the light-rays' deflection, the end points of the rays on the screen have to be located by using a reference pattern. The most often used reference pattern is the fringe pattern: a pattern with many parallel stripes, whose intensity follows a periodic intensity cosine function that corresponds to the coordinates of the pattern  $(x, y)$ :

$$i_0(x, y) = b(x, y) * \cos[2\pi f_0 + \varphi] \quad (1)$$

where  $i_0(x, y)$  is the intensity of the original pattern at  $x, y$  screen position,  $b(x, y)$  is the amplitude,  $f_0$  is the frequency and  $\varphi$  is the initial phase of the cosine function.

In order to calculate the deflection of the light- rays, the pattern's phase values for the camera pixels have to be evaluated. There are different methods for this task, the most wide spread are the phase-shift method (PSM), that is known from the interferometry, and the Fourier-transform method (FTM). PSM operates with a sequence of several instances of the same reference pattern, each shifted by a defined phase value, usually a fraction of a half period ( $\pi$  radians), and the camera captures an image of the object at each different phase. There are different versions of PSM based on the number (3-11) of patterns used for the evaluation. Since PSM needs a sequence of multiple images, care has to be taken, that the relative positions of the system's components: screen, object, and camera, stay constant during the capture of the whole image sequence, which needs vibration free environmental conditions. By the PSM, the evaluation of the phase values is done independently for each camera pixel, no coherence between the neighboring points is analyzed, and thus this method is noise sensitive.

The FTM was introduced by Takeda et al. [4], and Massig [5] used this method successfully for the evaluation of deflectometry data. FTM requires only a single camera image for the phase evaluation. All pixels of the camera image are analyzed together simultaneously as a whole, making this method robust against random noise or slight intensity changes in different spots of the image. Since the FTM can only obtain phase differences smaller than a period ( $-\pi \dots \pi$ ), it has to be combined with a phase unwrapping method, in order to calculate larger phase shift values.

The camera image with the distorted, eventually noisy pattern can be written in the following form:

$$i(x, y) = a(x, y) + b(x, y) * \cos[\Phi(x, y)] \quad (2)$$

$$\Phi(x, y) = 2\pi(f_{0x} + f_{0y}) + \varphi + \phi(x, y) \quad (3)$$

where  $i(x, y)$  is the intensity of the camera image at  $x, y$  position,  $a(x, y)$  is the local background intensity eventually noise,  $b(x, y)$  is the amplitude and  $\Phi(x, y)$  is the local, distorted phase of the cosine function, that contains the undistorted carrier signal, described by its frequency  $f_{0x}$ ,  $f_{0y}$  in x and y direction, phase  $\varphi$  and the local phase shift  $\phi(x, y)$  due to the distortion of the pattern. The second part of equation 2 can be rewritten in complex form:

$$b(x, y) * \cos[\Phi(x, y)] = b(x, y) * \frac{e^{i(\varphi+\phi(x,y))} + e^{-i(\varphi+\phi(x,y))}}{2} = c(x, y) + c^*(x, y) \quad (4)$$

$$c(x, y) = \frac{1}{2} b(x, y) e^{i(\varphi+\phi(x,y))}, \quad c^*(x, y) = \frac{1}{2} b(x, y) e^{-i(\varphi+\phi(x,y))} \quad (5)$$

where  $c^*(x, y)$  is the complex conjugate of  $c(x, y)$ . The camera image of the distorted reference pattern is transformed into the frequency domain via 2D Fourier-transformation:

$$I(f_x, f_y) = A(f_x, f_y) + C(f_x - f_{0x}, f_y - f_{0y}) + C^*(f_x + f_{0x}, f_y + f_{0y}) \quad (6)$$

where  $I(f_x, f_y)$ ,  $A(f_x, f_y)$ ,  $C(f_x, f_y)$  and  $C^*(f_x, f_y)$  are the Fourier transformed of  $i(x, y)$ ,  $a(x, y)$ ,  $c(x, y)$  and  $c^*(x, y)$  in the frequency domain. At this step the background  $a(x, y)$ , local variations  $b(x, y)$ , carrier wave and noise can be separated from the signal, based on their different frequencies by extracting the first order spectrum: selecting the spectrum around  $(f_{0x}, f_{0y})$  and translating it to the origin to get  $C(f_x, f_y)$ .

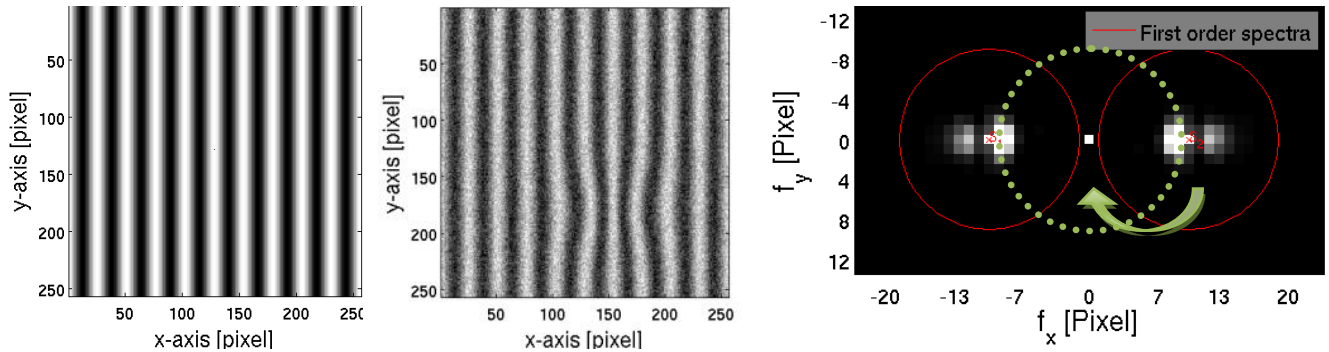


*Figure 2: a: original reference pattern, b: camera image: noisy, distorted reference pattern, c: Fourier-spectrum of the camera image*

The extracted spectrum is then inverse Fourier transformed, in order to get  $c(x, y)$ , from which, after deducting the known constant  $\varphi$ , the distortion due to the objects geometry  $\phi(x, y)$ , can be obtained as it is separated in the imaginary part:

$$\log[c(x, y)] = \log\left[\frac{1}{2} b(x, y)\right] + i(\varphi + \phi(x, y)) \quad (7)$$

The value of  $\phi(x, y)$  is wrapped between  $(-\pi$  and  $\pi)$ , thus an unwrapping operation can be necessary in case of larger distortions. In Figure 3 the original camera image with the noisy, distorted pattern and the evaluated phase difference can be observed.

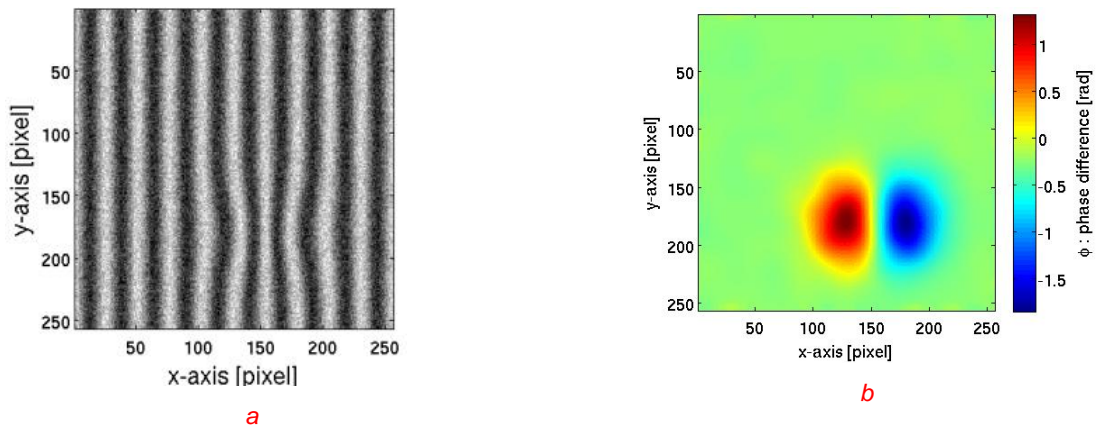


*Figure 3: a: Noisy, distorted pattern and b: its phase difference*

### SURFACE SCATTER

The deflectometry method requires specular reflecting surfaces. Observing a stripe pattern's reflection on a raw, aluminum, sheet metal surface, the camera image is blurred and noisy (see Figure 4b). With an increased display-object distance, which is necessary by larger object dimensions, the signal-to-noise ratio (SNR) of the pattern in the camera image worsens, till the signal is fully camouflaged by the noise, and thus even the noise tolerant FTM cannot be used anymore.

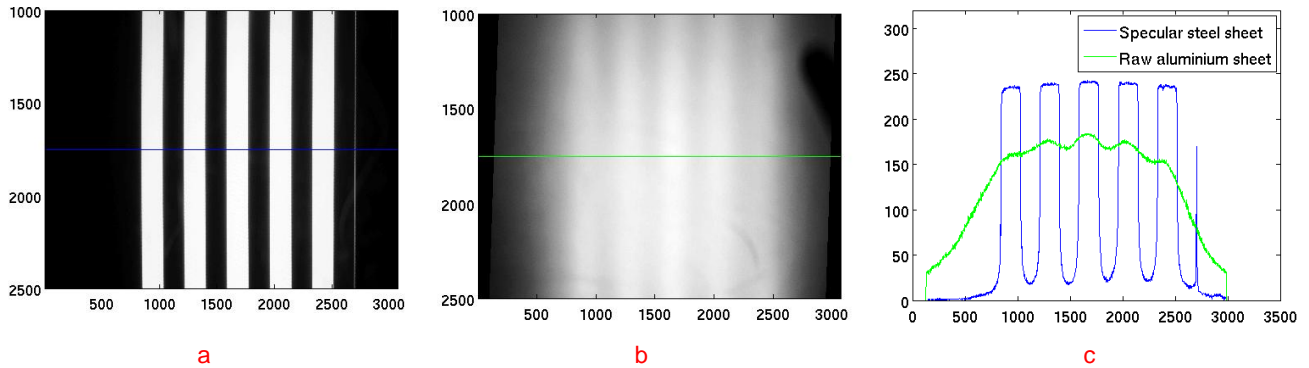


Figure 4. Reflection of a stripe pattern, displayed on a TFT (Thin Film Transistor) monitor at a distance of 250mm, from:  
 a. specular steel and b. raw aluminum sheet;  
 c. evaluation of intensities in the camera picture along same camera lines  
 (in case of raw aluminum the SNR is much lower than in case of specular steel)

The blur in the camera image is due to the surface scatter of the test object, which depends on the microstructure of the specimen's surface and the wavelength of the light. At microscopic levels, even the smoothest ones, consist of countless, tiny, randomly directed planar facets (see Figure 5a), that scatter incident light-rays in various directions. As the surface height's irregularity and frequency of peaks and valleys increase, the slope of the facets gets steeper, thus the divergence of the reflected light-rays will be larger.

Examining a single beam, a divergence of the parallel beam can be observed, after reflection from a surface (see Figure 5b), the reflected intensity is distributed under a solid angle, which is rendered as a blurry spot in the camera image (see Figure 5c). The camera image is an aggregate of lots of individual light-beams, which reach the elements of the camera's sensors and induce electric signals, and thus creating the image. From the camera's point of view, the scattering surface acts as a low pass filter on the image of the reference pattern, and the scattered image of the single beam is the kernel of the filter, termed as point spread function (PSF). Depending on the degree of scatter, rays from adjacent areas of the surface fall on the same sensor element, the sensor detects their summed intensity, which can be calculated by convolution (see equation 8).

$$i(x, y) = \int_{k=-\infty}^{\infty} \int_{l=-\infty}^{\infty} PSF(k, l) h(x - k, y - l) dk dl \quad (8)$$

where  $i(x, y)$  is the intensity detected by the camera at point  $(x, y)$ ,  $PSF(k, l)$  is the value of PSF at point  $(k, l)$  and  $h(x - k, y - l)$  is the intensity of the sharp image at point  $(x - k, y - l)$ . The PSF's size and distribution defines the filtering effect: the larger the area the PSF spreads on, the fainter and blurrier the resulted reflected image is. Since the PSF depends on the divergence of the beams, it also influenced by the distance between the camera and the scattering surface: The larger the distance between the camera and the object is, for example in case of a large object, the larger the PSF is, resulting a blurrier camera image.

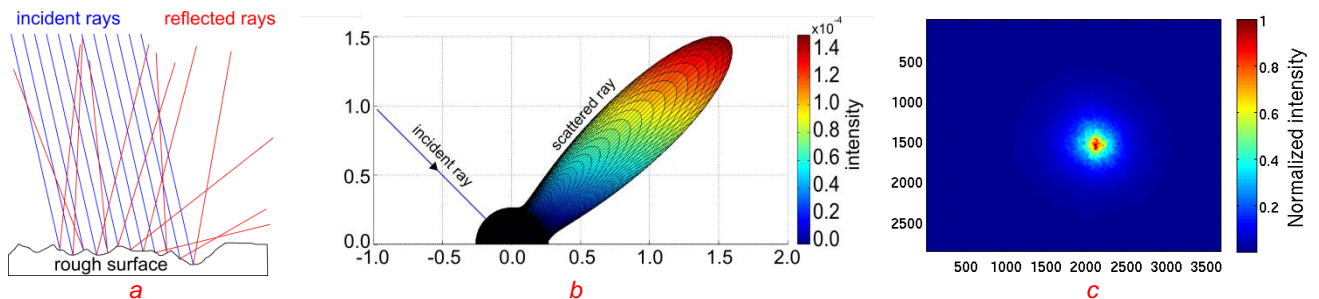


Figure 5. Scatter from rough surfaces: a. zoomed 2D scheme, b. 3D scatter of a light-beam (simulation), c. normalized distribution of intensity in a camera image reflected from a raw aluminum car-body

If the exact structure of the surface, i.e. each facet's direction, is known, the course of every single reflected light-ray can be determined. This kind of evaluation is very laborious, requires very precise measurements, and the scatter varies slightly at different positions of the surface. The microstructure of the surface is usually described by statistical parameters, like the RMS- (or  $R_q$ )-roughness (root mean square roughness), RMS-slope ( $m$ ), correlation length ( $\tau$ ) and probability distribution of the height irregularities, just to mention some of the most relevant ones that influence the facets' directions. The search for the correspondence between the statistical surface parameters and the scatter is the topic of many research studies. There are many different scatter models; some of them were made for rendering visually pleasing computer generated scenes, some for making physically correct calculations. We made beam scatter simulations using the He-Torrance-Sillion-Greenberg model [13] that is considered to be one of the most complex and physically correct one (see Figure 6). The scattered intensity of the reflected beam was simulated as it would be seen by a camera at a given distance, i.e. the PSF. It can be seen from the simulations that the scattering not only depends on the surface roughness parameters, but also on the wavelength of light, thus the increased degree of the scatter due to the roughness can be compensated by using longer wavelengths.

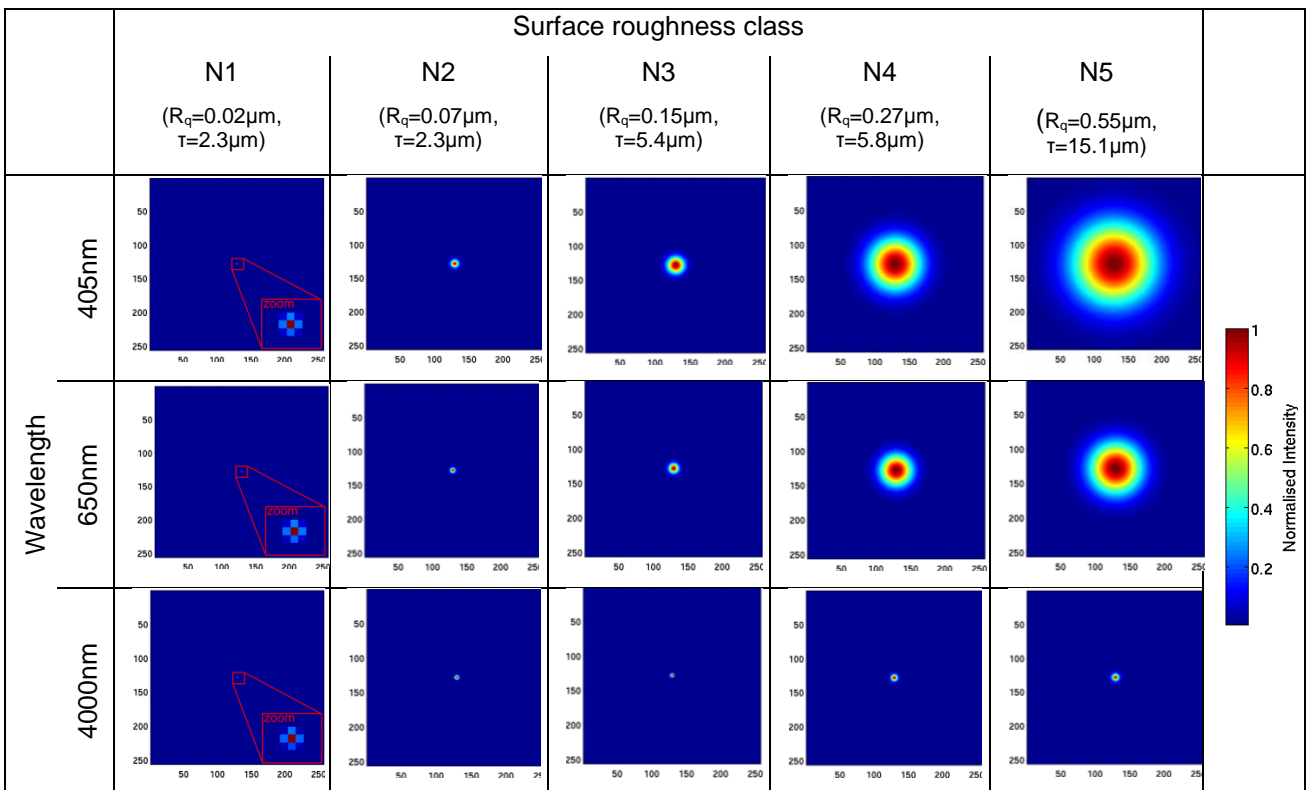


Figure 6: Simulation of scatter from surfaces with different roughness and at different wavelengths (additional sub-figures by column N1 magnification factor: 11.6x)

We also investigated the scatter of laser-beams via experiments with different wavelengths (red: 650nm and blue-violet: 405nm) from surfaces with different roughness. Among the tested specimens were different aluminum and steel parts. In Figure 7, a selection of 3 plain-ground steel roughness standards, so called Rugotests, can be seen with increasing roughness classes N1-N3. The parts were illuminated by a laser beam under a small  $5^\circ$  incident angle, the scattered beam fell on a white sheet of paper, which was captured by a digital camera. The exposure time and aperture of the camera was adjusted to the maximal intensity of the scattered beam, in order to avoid overexposed areas. The intensity of the captured images was normalized, in order to eliminate differences due to the intensity fluctuations of the beam. The results in Figure 7 are asymmetric due to the anisotropy of the ground surfaces; isotropic samples have central symmetric intensity distribution, like the ones in Figure 5c and Figure 6. From the results it can be seen as expected based on the simulations, that the degree of scatter increases with the height irregularity of the surface, and decreases with the wavelength of the beam.

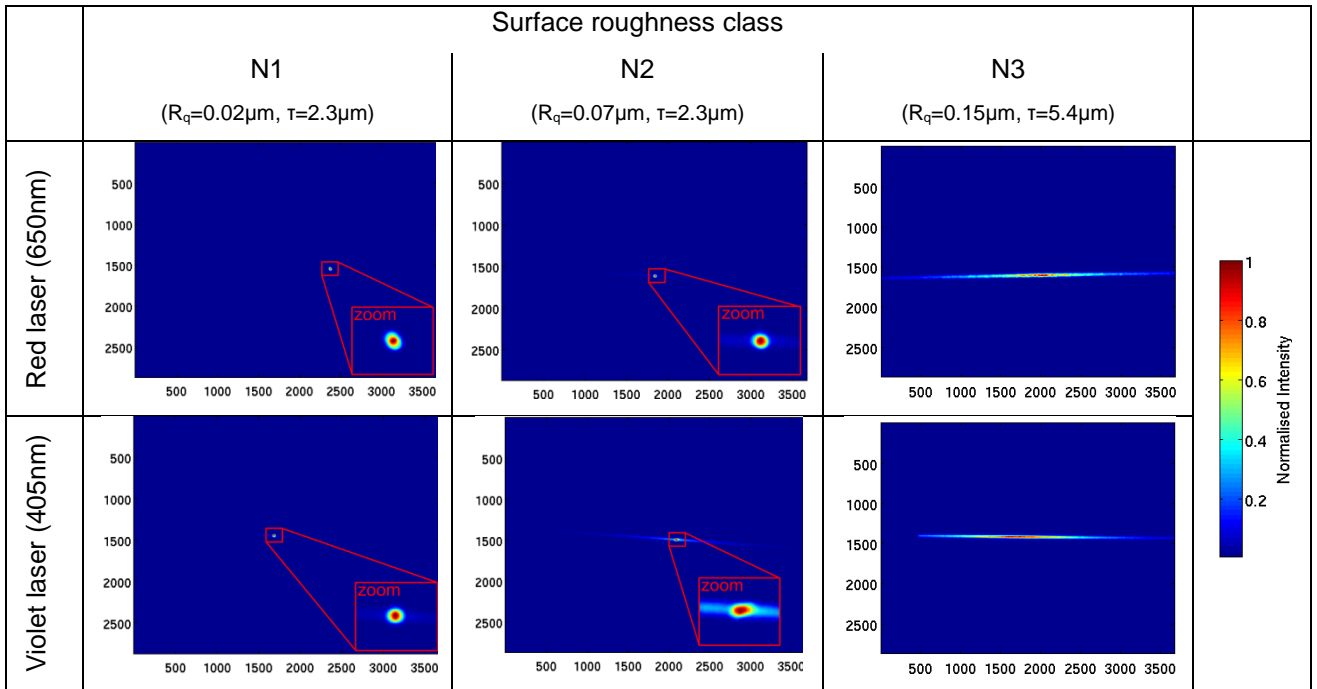


Figure 7: Scatter of laser beam at two different wavelengths (405nm and 650nm) from surfaces with different roughness, (additional sub-figure by column N1 and N2 magnification factor: 5x)

Measurements in the MWIR (Medium Wave Infrared) spectrum between 3.2 and 5 $\mu\text{m}$  wavelength were also made by using a thermo camera and a calibrated “Hohlraumstrahler” source. We measured the reflected radiation in a small solid angle, complying the specular reflection. The tests were made with the same parts that we used for the laser scatter tests. It was found, that in case of samples, where the RMS-roughness was smaller than 1/10th part of the light’s wavelength, the blur of the camera image was negligible. It agrees with the Rayleigh smoothness criterion: according to Rayleigh, the ratio between the wavelength of the light and the surface roughness for a smooth surface has to be larger than the following:

$$R_q < \frac{\lambda}{8 \cos \theta} \quad (9)$$

Where  $R_q$  is RMS roughness of the surface,  $\lambda$  is the wavelength of light, and  $\theta$  is the incident angle. If the wavelength of the light is much longer than the height irregularities of the surface, the scattering will be negligible and the surface can be considered smooth at that wavelength.

For more details about the reflection tests in the MWIR spectrum, please read 210-243-Sarosi [11].

### DEFLECTOMETRY IN THE INFRARED SPECTRUM

In order to reduce the filtering effect on the camera image, and to improve the SNR of the reference pattern’s image reflected from a large, rough surface, without using highlighting oil or other additional substances, the spectrum of the light used for the investigation has to be shifted from the visible to infrared spectrum. Both an imaging and a display device, capable of working at longer, infrared wavelengths, are needed for this kind of measurements. Nowadays, a wide range of infrared or thermo cameras are available, working at mainly in the MWIR (Medium Wave Infrared) and LWIR (Long Wave Infrared) atmospheric, infrared-windows between 3-5 $\mu\text{m}$  and 8-14 $\mu\text{m}$ . Beside the camera, a display device, capable of producing high-contrast images in the camera’s spectrum, is also needed.

Horbach [12] first used the increased specular reflectance of raw car-body parts in the LWIR range to make deflectometry measurements with a mechanically moved, static reference pattern. Static patterns are not very complicated to make, either the temperature, emissivity or transmittance of the display has to be changed according to the pattern in order to have an observable pattern in the infrared image. The drawback of these

techniques is that they can only display a static pattern: neither the texture nor the wavelength of the pattern can be changed.

In the visible range, there are many different, computer controlled display techniques: CRT (Cathode Ray Tube), TFT (Thin Film Transistor), plasma or projectors with screens, that can be used with deflectometry systems, though in the infrared range similar devices are not commercially available, since their only application field is in the military: testing the sensors and electronics of heat seeking missiles. We tested many different visible display techniques for infrared radiation (see Figure 8). A stripe pattern was displayed on each device. Unfortunately, no pattern was visible in case of CRT and TFT monitors, and in case of the plasma display the difference between the different lines was also negligible.

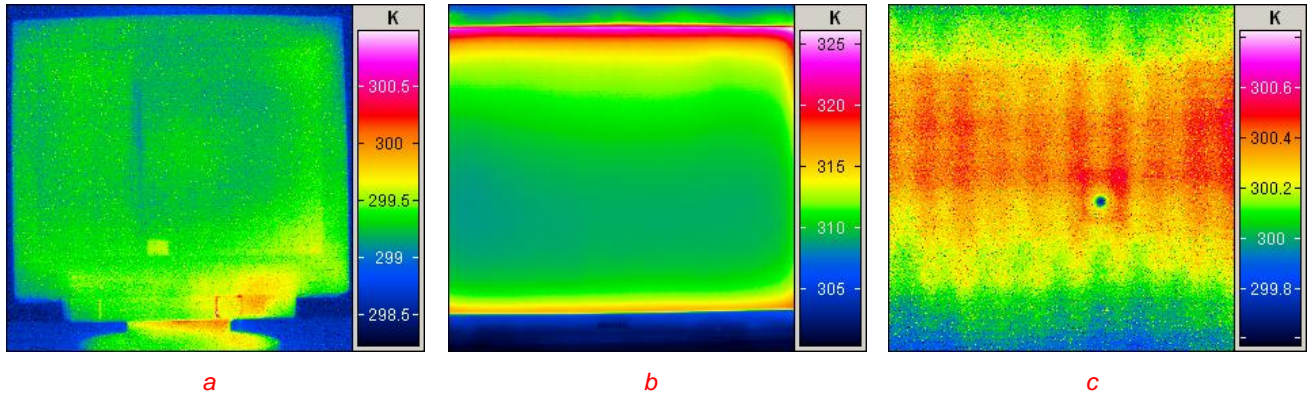


*Figure 8: Commercial displays in infrared spectrum a: CRT b: TFT c: Plasma*

We also made experiments with small test arrays of different electronic components: white LED (Light Emitting Diodes), SMD (Surface Mount Device) resistors and micro incandescent light bulbs (see Figure 9). The advantage of such a custom made constructions is, that using an electronic controller the current on the individual components of the array can be adjusted, thus the texture and the wavelength of the pattern can be changed easily and promptly.

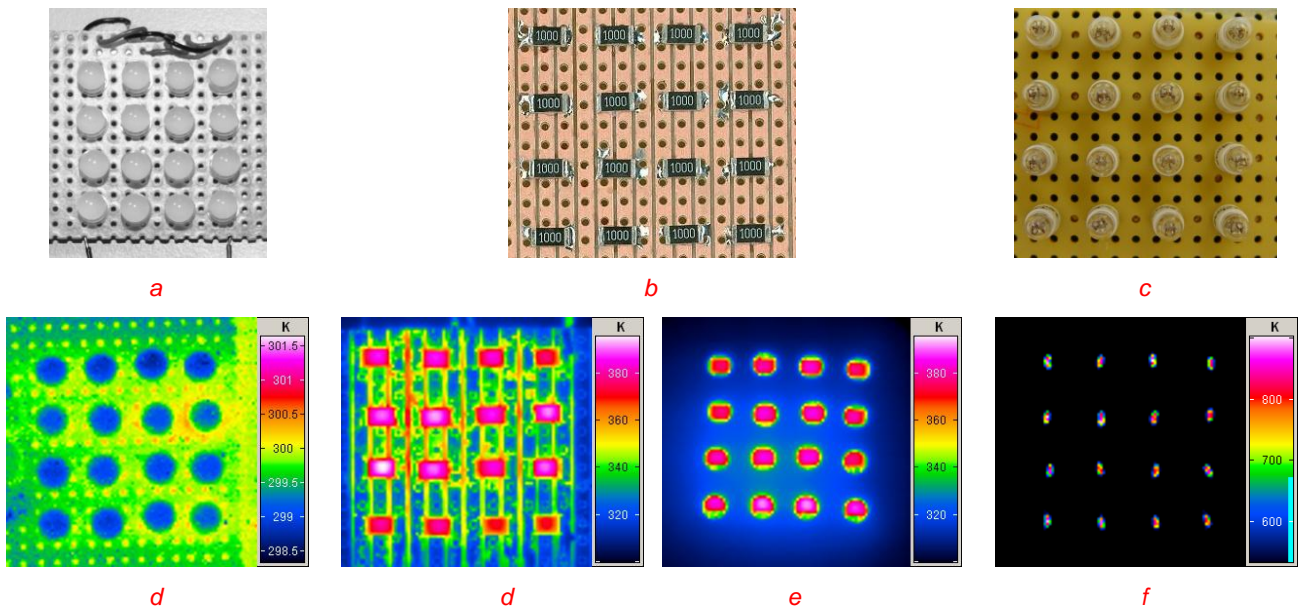


*Figure 9: Different arrays of electronic components and their infrared image: a,d: white LED, b,d,e: SMD resistors, (d: without, e: with mask), c,f: mini light bulb*

We found that in case of the LEDs the background produced more radiation than the LEDs itself due to the current (100mA) flowing through the wires on the backside of the panel. The SMD resistors can be heated slightly over 390K, but due to the current flow, and the heat convection of the copper wires on the panel, the background is also heated, spoiling the contrast of the pattern. Fortunately this can be easily solved by using a mask in front of the array. The highest temperature difference (>300K) was reached by using mini, incandescent light bulbs.

## EXPERIMENTS

We made experiments with a prototype IR display, consisting of a small matrix of incandescent light bulbs. The display was first tested from a distance of 40cm with a smooth gold plate in the visible spectrum (Figure 10a): the reflected image was clear and sharp, the first order spectra were clearly outstanding in the Fourier-domain. The same display was used from the same distance with a raw, aluminum, car-body part (Figure 10b). Here the matrix structure is not visible anymore, neither in the image nor in the frequency domain. The same sample was tested with the same display using a thermo camera at the wavelength 3.4-5 $\mu$ m: the matrix structure of the display appears, though not as clear as in case of the smooth gold plate, but still recognizable (Figure 10c). Using a thermo camera working at longer wavelengths, for example in the LWIR spectrum, even better results: higher contrast and sharper reflection images are expected due to the reduced scatter.

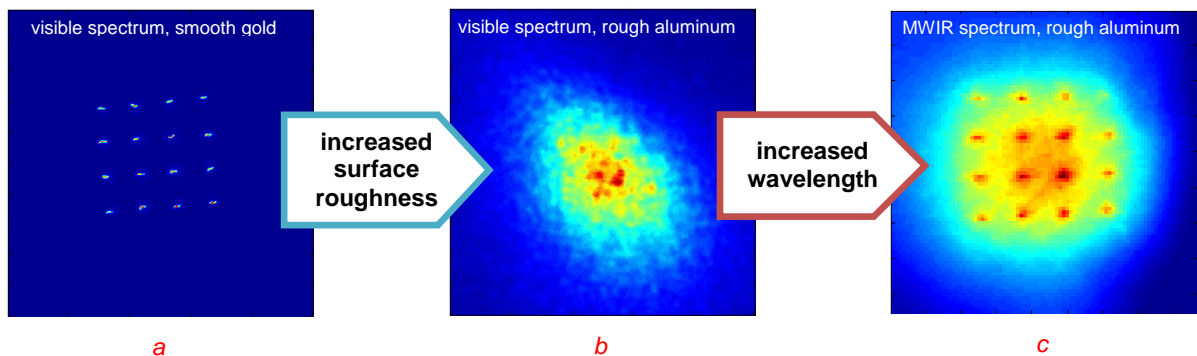


Figure 10. Reflection from a: smooth gold plate in visible spectrum, b: raw, aluminum car-body in visible spectrum, c: same as b. in MWIR spectrum

## SUMMARY AND OUTLOOK

Deflectometry is the appropriate method for the quick detection of small surface defects on large, smooth, specular reflecting objects, i.e. varnished car-body parts. Raw, unfinished car-body parts have a rough surface that scatters visible light. We use a thermo camera and a display capable of working in the infrared spectrum in order to shift the working spectrum to longer wavelengths, where the scatter of the surface is reduced, thus enabling the work with the deflectometry method. This way, the surface defects can be detected in the early stages of the manufacturing process, hence saving considerably time and costs. By applying the Fourier transform method, the evaluation of the measurement data can be made using a single exposure, increasing the vibration and noise tolerance of the system, which is vital in industrial environments. We are currently working on a large sized, dynamic, computer controlled infrared display to be able to make tests with real car-body parts. Comparative tests between the PSM and FTM methods will also follow to evaluate the noise tolerance, speed, vibration sensitivity of the two different methods. Substituting the MWIR camera by an LWIR model, we expect even better results in case of rough surfaces due to the reduced scatter.

## REFERENCES

- [1] Kühn B, Hrabal V, Brückner S, Lang GK, Traue HC. Physiologie und Psychologie der Wahrnehmung von Geometriefehlern auf Karosserieoberflächen. Universität Ulm; 1994.
- [2] Ritter R, Hahn R. Contribution to analysis of the reflection grating method. Optics and Lasers in Engineering. 1983;4(1):13-24.

- [3] Rose P, Surrel Y, Becker JM. Specific design requirements for a reliable slope and curvature measurement standard. *Measurement Science and Technology*. 2009;20(9):95110
- [4] Takeda M, Ina H, Kobayashi S. Fourier-transform method of fringe-pattern analysis for computer-based topography and interferometry. *Journal of the Optical Society of America*. 1982;72(1):156-160.
- [5] Massig JH. Deformation measurement on specular surfaces by simple means. *Optical Engineering*. 2001;40(10):2315-2318.
- [6] Tang Y, SU X, Liu Y, Jing H. 3D shape measurement of the aspheric mirror by advanced phase measuring deflectometry. *Opt. Express*. 2008;16(19):15090-15096.
- [7] Bothe T, Li W. 3D-Formvermessung per Streifenreflexion an Reflektoren für Autolampen (FRT). 2004:2-7.
- [8] Skydan OA, Lalor MJ, Burton DR. 3D shape measurement of automotive glass by using a fringe reflection technique. *Measurement Science and Technology*. 2007;18(1):106-114.
- [9] Liu L, Sawada T, Sakamoto M. Evaluation of the surface deflections in pressed automobile panels by an optical reflection method. *Journal of Materials Processing Technology*. 2000;103(2):280-287.
- [10] Bothe T. High-resolution 3D shape measurement on specular surfaces by fringe reflection. *Proceedings of SPIE*. 2004:411-422.
- [11] Sarosi Z, Knapp W, Kunz A, Wegener K. Evaluation of reflectivity of metal parts by a thermocamera. *Proceedings of InfraMation2010*. 210-243-Sarosi
- [12] Horbach JW, Kammel S. Deflectometric inspection of diffuse surfaces in the far-infrared spectrum. *Proceedings of SPIE*. 2005;5679(0):108-117.
- [13] He XD, Torrance KE, Sillion FX, Greenberg DP. A comprehensive physical model for light reflection. *ACM SIGGRAPH Computer Graphics*. 1991;25(4):175-186.

## **ABOUT THE AUTHOR**

The author received his MSc. degree in informatics in 2001 at the University of Miskolc, Hungary. He is currently working on his PhD. thesis in the field of optical metrology at the ETH Zurich in Switzerland while working for the inspire AG in Zurich. His main fields of interests are image processing, simulations and 3D optical measurement.